

NEW TEMPLATING ROUTE FOR SYNTHESIS OF MESOPOROUS ALUMINA

Naděžda ŽILKOVÁ^{a1}, Jiří ČEJKA^{a2}, Nataliya MURAFa^b and Arnošt ZUKAL^{a3,*}

^a J. Heyrovský Institute of Physical Chemistry, Academy of Sciences of the Czech Republic, v.v.i., Dolejškova 3, CZ-182 23 Prague 8, Czech Republic; e-mail: ¹ nadezda.zilkova@jh-inst.cas.cz, ² jiri.cejka@jh-inst.cas.cz, ³ arnost.zukal@jh-inst.cas.cz

^b Institute of Inorganic Chemistry, Academy of Sciences of the Czech Republic, v.v.i., CZ-250 68 Řež u Prahy, Czech Republic; e-mail: murafa@iic.cas.cz

Received April 23, 2008

Accepted July 3, 2008

Published online October 3, 2008

Synthesis of mesoporous alumina made by nanocasting using polymer spheres matrix is reported. In contrast to all other recipes described in the literature so far, mesoporous alumina prepared by the nanocasting method consists of irregularly ordered particles exhibiting pores of ca. 25 nm in size. The void volume among the particles constitutes a porous system with narrow pore size distribution in the mesopore region.

Keywords: Mesoporous alumina; Sphere templating route; Nanocasting.

Porous alumina is a very important material extensively used in catalysis, adsorption and other host-guest processes¹. Following the discovery of templated mesoporous silicates and aluminosilicates in 1992², the synthesis of organized mesoporous alumina with controlled mesoporosity was pursued³. In the literature one can find a number of reports discussing different approaches to the synthesis of mesoporous alumina based on “soft” templating routes using various “cationic”, “anionic” and “non-ionic” surfactants or ionic liquids in organic or aqueous solvents⁴⁻⁷. The state-of-the-art of supramolecular assembling, characterization and application potential of mesoporous alumina have been discussed in detail in the review⁸. An overview of mesostructured forms of alumina with crystalline framework walls has been reported elsewhere⁹.

As a result, different synthetic strategies provide in general more or less organized mesoporous aluminas mainly of a wormhole-like structure, with specific surface areas up to 500–600 m² g⁻¹ and void volume below 1 cm³ g⁻¹. The typical pore diameters reach 3–4 nm for the syntheses per-

formed with anionic surfactants, while large pores (6–10 nm) can be obtained using “neutral” routes with triblock copolymers¹⁰.

Large surface area, void volume and narrow pore size distribution of organized mesoporous alumina are the most important differences from conventional alumina. Hence, mesoporous aluminas offer interesting application as catalyst supports³. Several interesting examples of catalytic applications of organized mesoporous aluminas have already been described in the literature. After modification with MoO₃ or Re₂O₇, using the “thermal spreading method”, organized mesoporous aluminas showed some potential in hydrodesulfurization of thiophene or dibenzothiophene over MoO₃^{11,12} and in metathesis of linear olefins or unsaturated esters and ethers over Re₂O₇ catalysts^{13–15}.

Recently, a nanocasting route was developed, involving carbon aerogel as a “hard” template and aluminum nitrate as an alumina precursor¹⁶. Later on, an ordered crystalline alumina molecular sieve was prepared via nanocasting route using the same alumina precursor and mesoporous carbon replicated from hexagonal SBA-15 silica as a template¹⁷. However, sphere templating method permitting the formation of periodic porous solids¹⁸, has not been used so far for the preparation of mesoporous alumina. To our best knowledge, this is the first report describing the synthesis of mesoporous alumina based on this approach.

EXPERIMENTAL

Mesoporous alumina was synthesized by nanocasting using a polymer sphere matrix. The matrix was prepared from a polymer sphere suspension (copolymer of methyl methacrylate (90%) and 2-hydroxyethyl methacrylate (10%), diameter ca. 108 nm) by gravitational settling combined with drying at ambient temperature. The sedimentation relying on gravity and evaporation of the solvent made it possible to avoid densification of the sphere array. Dry plates prepared in this way were impregnated for 48 h in aqueous aluminum chloride hydroxide solution (Reheis, 28% Al, 50 wt.% solution), recovered by filtration and wetted by 25% NH₄OH solution (Fluka). Wet plates were kept in NH₃ atmosphere at ambient temperature for 24 h to hydrolyze aluminum chloride hydroxide. The prepared material was dried at 333 K overnight and calcined at 843 K for 12 h (temperature ramp 1 K min⁻¹).

The synthesized mesoporous alumina was characterized by X-ray powder diffraction (XRD), mercury porosimetry, nitrogen adsorption and high-resolution transmission electron microscopy (HRTEM) combined with electron diffraction (ED). XRD data were recorded on a Bruker D8 X-ray powder diffractometer equipped with a graphite monochromator and position sensitive detector (Vântec-1) using CuK α radiation (40 kV, 30 mA) in the Bragg-Brentano geometry.

Mercury intrusion experiments were performed over a wide range of pressures, starting from vacuum to over 400 MPa, using a Micromeritics Auto Pore III 9410 instrument. Prior to the pore structure analysis, the sample was degassed at 423 K overnight. Nitrogen sorp-

tion isotherm was measured with a Micromeritics ASAP 2020 volumetric instrument at 77 K. In order to attain a sufficient accuracy in the accumulation of the adsorption data, the instrument was equipped with pressure transducers covering the 133 Pa, 1.33 kPa and 133 kPa ranges.

Before sorption measurement, the sample was degassed, using a special heating program allowing for a slow removal of most preadsorbed water at low temperatures. This was done to avoid a potential structural damage of the sample due to surface tension effects and hydrothermal alternation. Starting at ambient temperature, the sample was degassed at 383 K (temperature ramp 0.5 K min^{-1}) until the residual pressure of 0.5 Pa was obtained. After further heating at 383 K for 1 h, the temperature was increased (temperature ramp 1 K min^{-1}) until the temperature of 523 K was achieved. This temperature was maintained for 8 h.

HRTEM images and ED patterns were obtained with a JEOL JEM-3010 instrument operating at an accelerating 300 kV voltage, using a LaB6 cathode. The samples were ultrasonically dispersed in ethanol and then dropped on the carbon-coated copper grids prior to the measurements.

RESULTS AND DISCUSSION

Figure 1 shows nitrogen adsorption isotherm on the prepared alumina. The isotherm reveals a type H1-hysteresis-loop, which is associated with porous materials characterized by narrow pore size distribution¹⁹. The BET surface area of $188.5 \text{ m}^2 \text{ g}^{-1}$ was calculated using data in the relative pressure range from 0.05 to 0.25. The pore size distributions (Fig. 2) were calculated both from nitrogen adsorption and mercury intrusion data. The mesopore distribution, obtained from the desorption branch of nitrogen isotherm using

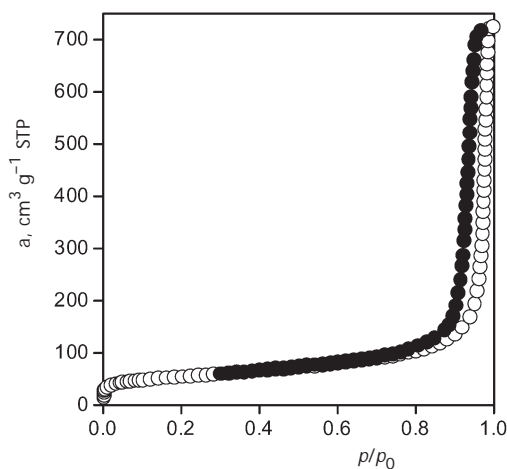


FIG. 1

Adsorption (○) isotherm of nitrogen on mesoporous alumina at 77 K (● desorption)

the Barrett-Joyner-Halenda (BJH) method, is centred at a diameter (D) of 25.7 nm; the corresponding mesopore volume (V) attains $1.013 \text{ cm}^3 \text{ g}^{-1}$. The pore size distribution obtained from mercury intrusion reveals the presence of mesopores and macropores. The volume of macropores with diameter larger than ca. $5.6 \mu\text{m}$ equals $0.193 \text{ cm}^3 \text{ g}^{-1}$. The distribution of mesopores is centred at 22.0 nm and their volume is $1.106 \text{ cm}^3 \text{ g}^{-1}$. It is clear that in the mesopore range, where the nitrogen adsorption and mercury intrusion overlap, both methods show a reasonable agreement. This agreement is very important, as both methods apply very different principles and, especially, the mercury porosimetry approach carried out under very high pressures could destroy the sample under study.

The crystallinity and morphology of the prepared alumina were examined by XRD, HRTEM and ED. Figure 3 displays an XRD pattern indicating a non-ordered overall character of alumina. The HRTEM image in Fig. 4 shows that the alumina sample consists of $\sim 20\text{-nm}$ particles. These nanoparticles are irregularly ordered; however, the voids among them constitute a porous system of narrow pore size distribution. A detailed inspection of HRTEM images has revealed that some of the particles feature a crystalline structure (Fig. 5). A typical ED pattern obtained from such local diffraction area is shown in Fig. 6. Three strong diffraction rings correspond to the (311), (411) and (440) planes of $\gamma\text{-Al}_2\text{O}_3$ ⁹.

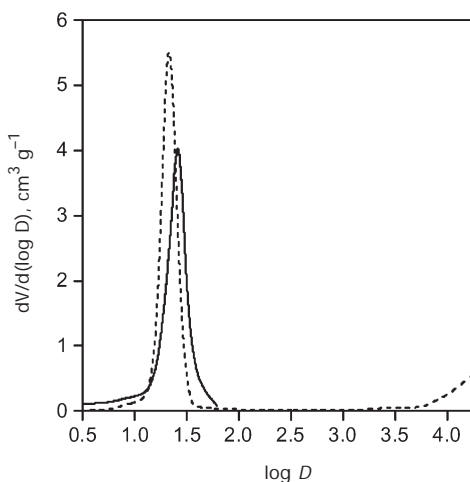


FIG. 2

Pore size distribution calculated from the desorption branch of nitrogen isotherm (solid line) and obtained by mercury porosimetry (dotted line). D (in nm) stands for mesopore diameter, V for mesopore volume

As shown above, the preparation of alumina involves three steps. In the first step, the template was prepared from dry plates obtained from colloidal spheres. In the second step, the pores of this template were filled with the aluminum chloride hydroxide solution, which was subsequently converted to a solid phase. The filling of template pores and the hydrolysis of aluminum chloride hydroxide were performed only once. Therefore, the template pores were not fully filled with the alumina precursor and the cal-

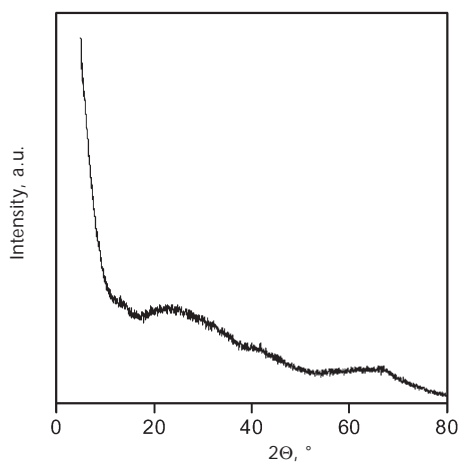


FIG. 3
XRD pattern of mesoporous alumina

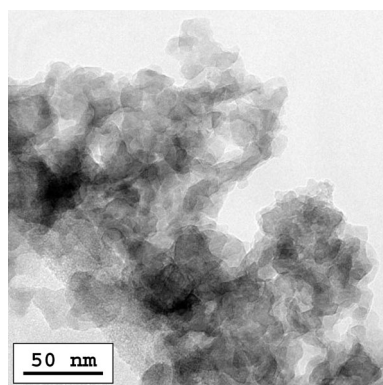


FIG. 4
HRTEM image of mesoporous alumina

cination in the third step resulted in pronounced shrinkage of the solid phase. A comparison of the polymer sphere size and the pore size shows that the shrinkage attains ca. 80%. As the shrinkage occurs to such extent, the ordering of the original skeleton is destroyed. However, the narrow distribution of the pores, which were templated by monodisperse polymer spheres, is preserved.

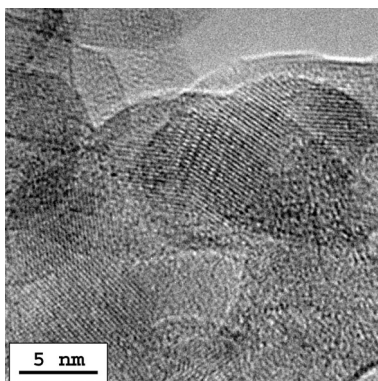


FIG. 5
HRTEM image of selected particles of mesoporous alumina

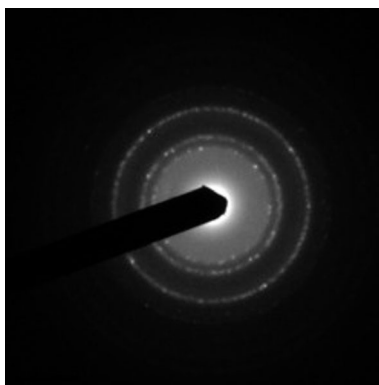


FIG. 6
ED pattern of mesoporous alumina (selected area)

In conclusion, organized mesoporous alumina with mesopores around 20–25 nm possessing a narrow pore size distribution was synthesized using the nanocasting method. For this purpose, spheres of the methyl methacrylate (90%)–2-hydroxyethyl methacrylate (10%) copolymer were used.

The resulting mesoporous alumina exhibits the BET surface area close to $200 \text{ m}^2 \text{ g}^{-1}$ and the void volume larger than $1 \text{ cm}^3 \text{ g}^{-1}$. The mesopore distribution obtained from the desorption branch of nitrogen isotherm using the BJH method is centred at a diameter of 25.7 nm while mercury porosimetry provided a value of ca. 22 nm. Both methods show a good agreement.

X-ray powder diffraction at a wide range of diffraction angles evidenced mostly the amorphous character of this type of alumina, without a particle ordering on the microscale level.

The authors acknowledge the financial support of the Grant Agency of the Academy of Sciences of the Czech Republic (A400400805) and of the European Community STREP project "DeSANNs" (No. FP6-SES6-020133).

REFERENCES

1. Misra C. (Ed.): *Industrial Alumina Chemicals*, Chap. 1, ACS Monograph 184. American Chemical Society, Washington D.C. 1986.
2. Kresge C. T., Leonowicz M. E., Roth W. J., Vartuli J. C., Beck J. S.: *Nature* **1992**, 359, 710.
3. Márquez-Alvarez C., Žilková N., Pérez-Pariente J., Čejka J.: *Catal. Rev.* **2008**, 50, 222.
4. Vaudry F., Khodabandeh S., Davis M. E.: *Chem. Mater.* **1996**, 8, 1451.
5. Čejka J., Kooyman P. J., Veselá L., Rathouský J., Zukal A.: *Phys. Chem. Chem. Phys.* **2002**, 4, 4823.
6. Žilková N., Zukal A., Čejka J.: *Microporous Mesoporous Mater.* **2006**, 95, 176.
7. Ray J. C., You K.-S., Ahn J.-W., Ahn W.-S.: *Microporous Mesoporous Mater.* **2007**, 100, 183.
8. Čejka J.: *Appl. Catal., A.* **2003**, 254, 327.
9. Pinnavaia T. J., Zhang Z., Hicks R. W.: *Stud. Surf. Sci. Catal.* **2005**, 156, 1.
10. Zhang Z., Pinnavaia T. J.: *J. Am. Chem. Soc.* **2002**, 124, 12294.
11. Kaluža L., Zdražil M., Žilková N., Čejka J.: *Catal. Commun.* **2002**, 3, 151.
12. Hicks R. W., Castagnola N. B., Zhang Z. R., Pinnavaia T. J., Marshall C. L.: *Appl. Catal., A* **2003**, 254, 311.
13. Balcar H., Hamtil R., Žilková N., Čejka J.: *Catal. Lett.* **2004**, 97, 25.
14. Hamtil R., Žilková N., Balcar H., Čejka J.: *Appl. Catal., A* **2006**, 30, 193.
15. Balcar H., Hamtil R., Žilková N., Zhang Z., Pinnavaia T. J., Čejka J.: *Appl. Catal., A* **2007**, 320, 56.
16. Li W.-C., Lu A.-H., Schmidt W., Schüth F.: *Chem. Eur. J.* **2005**, 11, 1658.
17. Liu Q., Wang A., Wang X., Zhang T.: *Mater. Chem.* **2006**, 18, 5153.
18. Stein A.: *Microporous Mesoporous Mater.* **2001**, 44–45, 227.
19. Lowell S., Shields J. E., Thomas M. A., Thommes M.: *Characterization of Porous Solids and Powders: Surface Area, Pore Size and Density*, p. 43. Kluwer Academic Publishers, Dordrecht 2004.